https://doi.org/10.1016/j.nanoen.2018.10.073

Strategies and progress on improving robustness and reliability of triboelectric nanogenerators

*Wei Xu, Man-Chung Wong, Jianhua Hao**

W. Xu, Man-Chung Wong, Prof. J. H. Hao,

Department of Applied Physics, The Hong Kong Polytechnic University, Hong Kong, P. R. China

E-mail: jh.hao@polyu.edu.hk

Abstract

Triboelectric nanogenerator (TENG) is a novel technology converting mechanical energy into electricity and has shown great potential in coping with energy and environmental crisis, and driving emerging electronics. The robustness and reliability represent the ability of TENGs to conduct long-term, stable, and reliable operation, and are considered as the precondition for realizing the extensive and large-scale application of this device in realistic environment. However, the robustness and reliability of TENGs are being severely challanged by frequent, direct and long-term mechanical impacts as well as negative environmental factors during the operation of device. Therefore, how to improve the robustness and reliablity of TENGs is an important issue that urgently need to be addressed. In this article, we review five types of feasible strategies, including noncontact mode, rolling structural, liquid-solid

contact, self-recovery and encapsulated TENGs, for the enhancement of robustness and reliability. Some representative examples and their merits are highlighted and demonstrated. The contribution, availability, and challenges toward each strategy are discussed.

Keywords: Triboelectric nanogenerators, Robustness, Reliability, Mechanical energy harvesting

1. Introduction

With the rapid progress of human civilization, the current energy supply situation is facing improvedly severe challenge. On the one hand, the huge consumption of limited fossil energy leads to the threat from the energy exhaustion and global warming [1-3]. On the other hand, recently overwhelming development of emerging electronics urgently requires novel power supply technologies to overcome the shortcomings of traditonal power sources, such as limited lifetime, frequently replacing operation and safety hazard [4-7]. To cope with energy and environmental crisis, and meet the development requirement of emerging electronics, triboelectric nanogenerator (TENG), a novel technology converting ambient mechanical energy into electricity, was proposed and invented in 2012 by Zhong Lin Wang et al [8]. Compared to its counterparts, the TENG presents many distinctive advantages, including simple fabrication process, low-cost, various working modes, abundant choice of constituent materials and structures, and higher energy conversion efficiency in low frequency

range etc. [8-12], and has become an ideal alternative of traditional power technologies. Correspondingly, a series of TENGs have been fabricated and employed as sustainable power sources and self-powered sensors for various application [13-19].

The operation of TENGs is based on the conjunction of triboelectrification and electrostatic induction [4, 5, 20]. Specifically, when two different materials sufficiently contact, the charges (electrons, ions and molecules, etc.) will transfer at the interface to equalize the electrochemical potential between distinct materials. With the separation of the charged surfaces, triboelectric charges are generated on friction surfaces, leading to the electric potential difference between two electrodes attached on triboelectric materials by means of the electrostatic effect. This process is generally driven by mechanical force, and the mechanical energy therefore is converted into electricity [2, 20, 21]. On the basis of this operation mechanism, it is noticed that, to achieve the useable triboelectricity, the TENG has to suffer from frequent, direct and long-term mechanical impacts. This is prone to cause the material and device failures, generating a series of problems, such as the degradation of output performance, the loss of life-span, and safety hazard [22-24]. Even though some excellent and tough materials, such as polytetrafluoroethylene (PTFE), polyimides, and specially modified hybridizing micro-nanocomposite materials, have been employed to try to withstand this mechanical wear and the harsh operation environment [25], the TENG still shows a relatively lower robustness compared to its counterparts,

which seriously decreases its competitiveness. Meanwhile, some environmental factories, such as dust and moisture etc., also may negetively affect the performance of device by invading the surface of triboelectricity materials [26-28]. In this regard, developing some feasible strategies to improve the robustness and reliablity of TENGs is an important issue that urgently need to be addressed. Looking at it in another way, as a promising candidate for powering emerging electronics, the reliability and robustness of TENGs play crucial role for guaranteeing the long-term, stable, and reliable operation of these electronics, and are considered as the precondition realizing the extensive and large-scale application of TENGs in realistic environment [4, 5, 29]. Generally, the good reliability and robustness for TENGs represent that the device and the corresponding self-powered system should not only can provide steady output for long time in various operation environments, but also possess the ability of recovering the device to the normal working state in short time once a fail happens.

During the past a few years, a series of progress related to different aspects of TENGs ranging from fundamental study to application extension have been achieved and reviewed [5, 30-35]. However, up to now, there is no special review focusing on the topic of improving robustness and reliability of TENGs. In this article, we will review the contribution of five types of different technology strategies, including noncontact mode, rolling structural, liquid-solid contact, self-recovery and encapsulated TENGs, on the enhancement of robustness and reliability as illustrated in Fig. 1. Some representative examples and their merits are highlighted and

demonstrated. Finally, the availability, feature and challenges toward each strategy are briefly discussed, and some future perspectives are suggested.

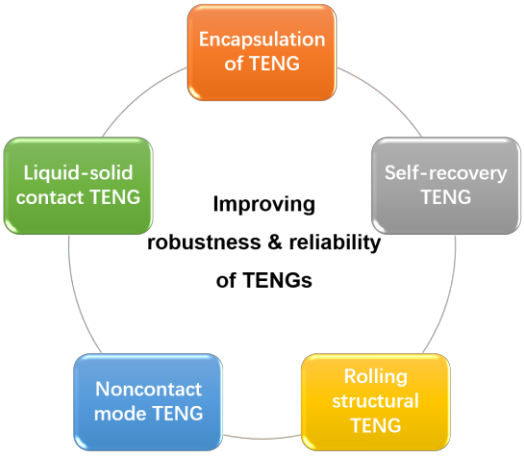

Fig. 1. Main strategies for improving robustness and reliability of triboelectric nanogenerators.

2. Noncontact mode TENG

Generally, there are four basic operation modes for TENGs, including the vertical contact-separation mode [13, 36-38], the lateral sliding mode [39-42], the single electrode mode [43-46], and the free-standing triboelectric layer mode [47-49], which are the basis for various TENGs prototypes. However, for all these modes, the operation of device requires the direct physical contact between two triboelectric materials for electricity generation, which will cause device abrasion and heat generation under continuous operation and thus degrade the robustness and reliability of device. This situation can be improved by introducing a new operation mode, namely noncontact mode [4, 47, 50, 51]. Specifically, in practical application, it is possible that the triboelectric layers have been pre-charged by either initial contact between triboelectric materials or friction with objects in natural surroundings in

advance [4, 5, 29]. These electrostatic charges are capable of remaining on the triboelectric layer surface for hours due to the insulation of at least one triboelectric material. Within this period, the charges flow at external circuit can be induced by relative motion between the per-charged triboelectric layers even without direct contact to further generate electricity, and a noncontact mode TENG therefore is formed.

Taking advantage of the concept of noncontact mode, many corresponding TENGs have been fabricated and shown the improved robustness. Lin et al. reported a noncontact free-rotating disk triboelectric nanogenerator (FRD-TENG) [50], in which two separated aluminum (Al) foils (4 inch in diameter) with complementary four-segment shapes act as the two stationary electrodes, and a piece of fluorinated ethylene propylene (FEP) thin film with the same four-segment structure serves as rotatable tribo-charged layer, as shown in Fig. 2a. The FEP is firstly charged by bringing the FEP layer and one Al foil into contact for charges transfer based on triboelectric effect. Accompany with the vertical separation of these two layers (0.5 mm in gap distance) and the subsequent noncontact relative rotation between the charged FEP and Al, the electrostatic charges preserved on the dielectric FEP surfaces will induce the electrons flow between two separated Al electrodes to create electricity as shown in Fig. 2b. The measured results elucidate that the prepared noncontact mode TENG can effectively convert mechanical energy into electricity without further friction, and the open-circuit voltage (V_{oc}) and the short-circuit current

density (J_{sc}) at 500 rpm can reach up to 220 V and 1.8 mA/m^2, respectively, with only slightly lower than those generated by the contact mode device. Most importantly, attributed to its unique noncontact operation, the FRD-TENG has excellent robustness and durability to avoid the degradation in both triboelectric materials and output performance, especially at very high rotation speed. Fig. 2c compares the SEM images of the FEP surface morphology at initial state and after 50 hr operation at a rotation speed of 3000 rpm, and no obvious surface wear in polymer is observed. Correspondingly, the output parameters (V_{oc} and J_{sc}) of the FRD-TENG with eight-segment structure (inset of Fig. 2d) were measured before and after a 500000-cycle continuous operation, and the device's output displays only little drops (Fig. 2d and 2e). These results indicate the super high durability and robustness of the noncontact device. Besides the mentioned FRD-TENG, noncontact mode TENGs with other structures, such as plate structure, rotating fan structure, or linear grating structures etc. were also reported for harvesting various mechanical energy from moving objects, human motion and acceleration of vehicles, or serving as non-contact electronic skin, and all of them perform an increased reliability and robustness [29, 47,49, 52, 53].

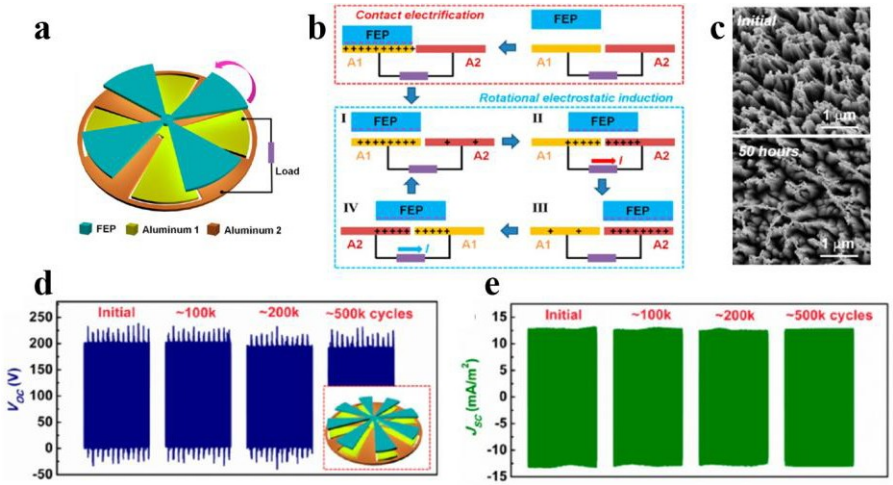

Fig. 2. (a) Device structure and (b) working principle of the noncontact free-rotating disk triboelectric nanogenerator (FRD-TENG). (c) The SEM images of the nanostructure on FEP triboelectric layer surface before and after a continuous operation for 50 hr. (d) Open-circuit voltage and (e) short-circuit current density of device before and after continuously operating for 100000, 200000, and 500000 cycles. Reproduced with permission from American Chemical Society [50].

For noncontact mode TENGs, the charges preserved on the surface of dielectric triboelectric-layers will gradually decay, leading to the decline of the electric output. This means that the operation of noncontact mode device has to been frequently interrupted for surface charge replenishment, which limits their practical applications. To address this concern, an TENG enabling the automatic transition between the contact and noncontact modes was demonstrated for wind energy harvesting [29]. As shown in Fig. 3a, the structure of entire device mainly includes two parts: the stationary outer barrel that connects with the Al stator disk of the TENG, and the rotational inner barrel connected with a freestanding FEP rotor disk of TENG by stopping ring. The rotor and stator disks possess the similar structure with the FRD-TENG mentioned in Fig 2a, and the stopping ring linkage (inset of Fig. 3a)

enables the axial movement of rotor disk even though during the relative rotation process between rotor and stator disks. The key of automatic transition between two modes is to create two opposite forces applied on the rotor disk. They include a force to pull the rotor to close to the stator from one tensile spring connecting the rotor disk with the bottom of inner barrel, and an opposite push force that prefers driving the rotor disk apart from the stator by a fan attached to the rotor with four rectangular blades tilted by 35°, as depicted in Fig. 3b. The theoretical and experimental relationships between the short-circuit transfer charge ($,,1Q_{sc}$) and wind speed are illustrated in Fig. 3c and 3d, respectively. It is found that the TENG works in contact mode at low wind speed. With the wind speed increases, the fast rotation of fan provides an increased push force to vertically separate rotor from the stator disk. Correspondingly, the contact mode automatically transforms into the noncontact mode until the wind speed is decreased where the device returns to contact mode. By means of this process, the TENG can mainly work in noncontact mode without abrasion and occasionally transit into contact mode for the surface charge replenishment, which specially suits harvesting energy of natural wind with a fluctuating speed. Long-term tests for the automatic mode transition TENG reveal that after 120000 rotation cycles, the nanostructures on the FEP rotor surface suffer from a minimized surface wear with only about 5% performance degradation in $,,1Q_{sc}$ (Fig. 3e and 3f). In contrast, the FEP surface nanostructures in contact mode TENG have been almost completely wiped out and the $,,1Q_{sc}$ degradation reaches up to 40% after only

24000 cycles (Fig. 3e and 3g). Thus, the automatic transition in modes brings TENGs a significant improvement in both robustness and practicability. Besides, even though most reported noncontact TENGs operate by means of the relative motion of charged triboelectric layers in parallel direction, such as sliding, it is also feasible to create the electric signals by the noncontact vertical motion between charged triboelectric layers with distance change. The corresponding noncontact devices have been fabricated as the energy harvester, self-powered vibration sensor, and speedometer with higher reliability [54, 55].

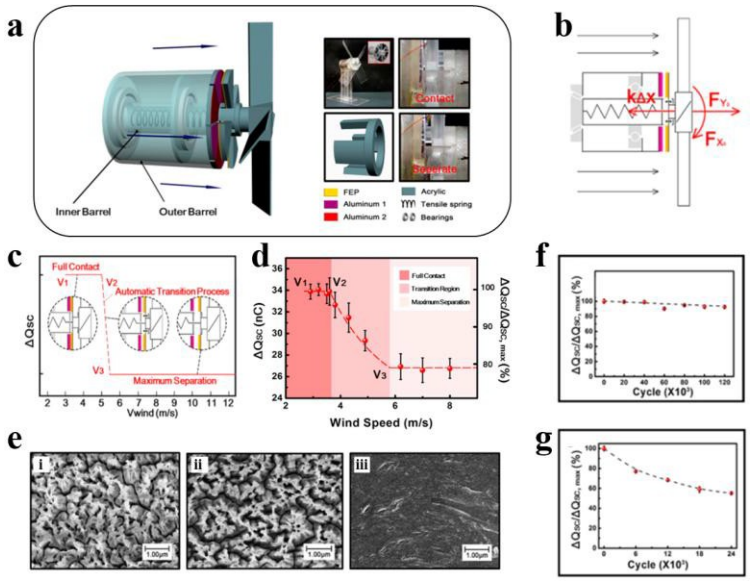

Fig. 3. (a) The schematic of the whole device. The insets successively include the photograph of device, the structure of the stopping ring, and the amplified images of the disk TENG in contact and noncontact state. (b) The force analysis for the movable rotor disk. (c) Theoretical and (d) experimental relationship between the short-circuit transfer charge ($,,1Q_{sc}$) and wind speed. (e) SEM images of FEP surface nanostructures at initial state, after operating at noncontact mode for 120000 rotation cycles and after operating at contact mode for 24000 rotation cycles. (e) and (f) $,,1Q_{sc}$ /$,,1Q_{sc,\ max}$ change with operating the device at noncontact mode (f) and at contact mode (g), where $,,1Q_{sc,\ max}$ is the initial $,,1Q_{sc}$. Reproduced with permission from American Chemical Society [29].

The aforementioned noncontact mode TENGs focus on preventing the physical contact between two triboelectric materials for relieving device abrasion. Similarly, the robustness of device can also be enhanced by avoiding the direct impact of external mechanical force on TENGs. For instance, our group reported a magnetic-assisted noncontact TENG by coating a magnetic response polymer composite layer on the surface of device (Fig. 4a (i)) [56]. As a result, the interaction between triboelectric materials, including Al and PDMS (Fig. 4a (ii)), in device can be remotely controlled by the motion of external magnet via magnetic field mediation to generate electricity (Fig. 4a (iii)). This design avoids the direct contact between device and external mechanical stimuli in traditional TENGs and therefore delays the device degradation and failure. Meanwhile, such a magnetic-assisted noncontact TENG shows the potential to convert some complicated and random external mechanical motions into a simple contact-separation between triboelectric materials, which benefits the improvement in usability, stability, and reliability of generated triboelectricity. These advantages enable the device to be appropriate for harvesting nature wind and water energy with random speed, frequency, and amplitude (Fig. 4b) [57]. Moreover, a similar magnetic force driven noncontact hybrid electromagnetic-triboelectric nanogenerator has been reported using the electrospun Fe_3O_4 nanoparticles embedded PVDF fibers membrane as the magnetic responsive layer as shown in Fig. 4c [58].

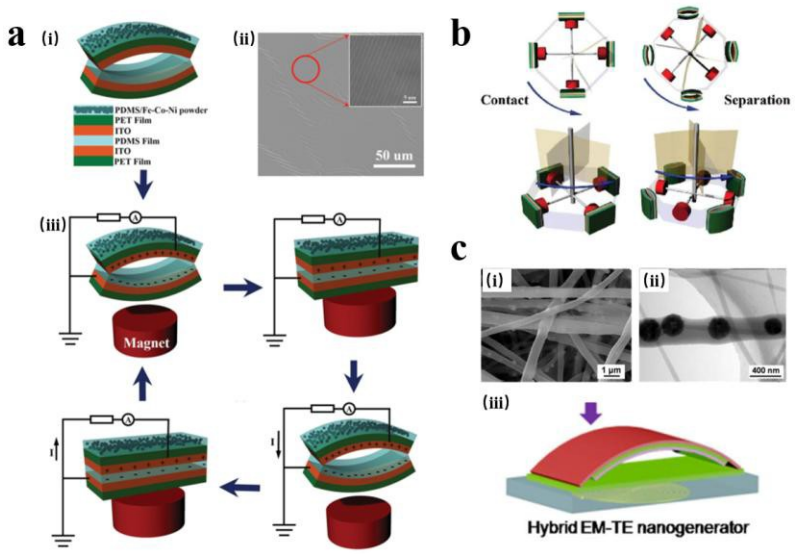

Fig. 4. (a) Device structure (i), the surface microstructure of PDMS triboelectric layer, and the working principle (iii) of the magnetic-assisted noncontact TENG. Reproduced with permission from Wiley-VCH [56]. (b) The application of the magnetic-assisted noncontact TENG for wind and water energy harvesting. Reproduced with permission from Elsevier [57]. (c) SEM (i) and TEM (ii) image of Fe_3O_4 nanoparticles embedded PVDF fibers as the magnetic responsive layer of the magnetic force driven noncontact hybrid electromagnetic-triboelectric nanogenerator (iii). Reproduced with permission from Elsevier [58].

In summary, fabricating the noncontact mode TENGs is a straightforward and effective method to reduce the device abrasion because the contact and friction between triboelectric materials or between external force and device are completely avoided. However, for the same reason, the electric output of noncontact mode TENG is usually smaller than that generated by its counterpart operating at contact mode. Besides, the gradual decay of charges preserved on the surface of dielectric triboelectric layers is another factor to limit the effective operation of noncontact mode device. Although some TENGs enabling the automatic surface charge

replenishment were demonstrated, their relative complex device structure should be further optimized.

3. Rolling structural TENG

As aforementioned, one of the key factories to improve the robustness of device is to decrease the friction abrasion either between triboelectric materials or between mechanical stimuli and device. Based on this principle, a series of rolling-structural TENGs with the reduced frictional resistance between triboelectric surfaces have been reported for robust operation [59-64]. Fig. 5a illustrates a rolling triboelectric nanogenerators (RTENG) consisting of a group of rolling steel rods sandwiched by two layers of FEP thin films [61]. For each FEP layer, there is a pair of separated copper electrodes deposited on its back side. During the operation process of the RTENG, the rolling motion of steel rods between the top and down FEP layers creates triboelectric charges on contact surfaces due to their distinct electron affinity. The rolling of charged rods will further lead to the potential difference between separated electrodes on the back of each FEP layer and drive the electrons flow in the external circuit as shown in Fig. 5b. Due to the normalized friction coefficient of the rolling friction of rods is measured substantially lower than that of the planar sliding friction (Fig. 5c (i)), the robustness and durability of the RTENG are obviously improved compared to traditional structural TENGs. Fig. 5c (ii)-(iv) compare the surface morphology change of the employed FEP triboelectric layer after undergoing the rolling and sliding friction of 1000 cycles. It is clearly observed that the sample

enduring rolling friction shows little degradation in the surface nanowire structures, while the other sample has been seriously destroyed. This demonstrates the unique advantage of the rolling structure in improve durability of TENGs compared to the traditional sliding TENGs. On the basis of this strategy of rolling structure, many other RTENGs have been successfully derived [59-63]. For example, Wang et al. reported a RTENG and electromagnetic generator (EMG) hybrid nanogenerator with negligible electrical output degradation after continuous rolling of more than 9000 cycles [65]. Similarly, another rolling friction contact-separation mode hybrid triboelectric nanogenerator has been fabricated by Yang et al. as shown in Fig. 5d [63]. Besides, some prototypes based on rolling balls instead of rods have also been fabricated with the rotating disk structure, the grating structure, the vortex whistle structure etc [59-61].

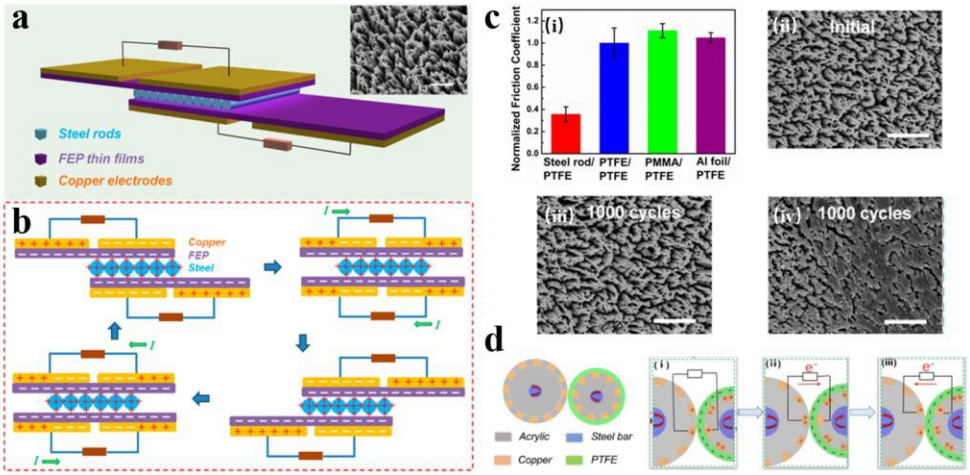

Fig. 5. (a) Structure and (b) working principle of the rolling triboelectric nanogenerator (RTENG). (c) Normalized friction coefficient comparison of the rolling friction and the planar sliding friction (i), and SEM images of FEP surface morphology at initial state (ii), and after operating at rolling friction (iii) and sliding friction (iv) for 1000 cycles. Reproduced with permission from American Chemical

Society [61]. (d) Structure and working principle schematics of a rolling friction contact-separation mode hybrid triboelectric nanogenerator. Reproduced with permission from Elsevier [63].

Given the low friction resistance of rolling motion, some attempts have been conducted to integrate the rolling structure with the noncontact mode TENGs to overcome the issue of electrostatic charge dissipation in common noncontact TENGs without compromising the device robustness. Guo et al. reported a rolling friction enhanced free-standing mode triboelectric nanogenerator (RF-TENG) as shown in Fig. 6a [66]. This design includes a rotor, a stator, and an Al rod. The stator is two sets of complementary patterned copper electrodes deposited onto the Kapton film (inset of Fig. 6a (i)). The rotor is a layer of paralleled identical copper stripes deposited onto a FEP thin film (inset of Fig. 6a (ii)) with nanowires pattern (inset of Fig. 6a (iii)). The rotor and the stator form a prototype of noncontact TENG. On the other hand, the rolling contact between the Al rod and the rotor will make both FEP and copper on rotor charged, which induces the charges flow between two electrodes on stator of RF-TENG through noncontact relative motion between stator and rotor as depicted in Fig. 6b. Compared to the common noncontact mode TENG (NC-TENG), the introduction of the rolling structural part can continuously replenish triboelectric charges into the rotor surface to remain a saturated charges level. This assures a maximized and constant electric power of TENGs. As shown in Fig. 6c, the electric output of device is doubled with the rolling-friction-induced charge replenishment. Most importantly, this high electric output of RF-TENG can hold constant after a

long-term operation as demonstrated in Fig. 6d. It is found that, after 14.4 million cycles of rotations, the output of RF-TENG only shows a minor fluctuation of less than 0.2%, while the output of NC-TENG decreases by about 15%. On the other hand, since the rolling friction causes almost no damage to the triboelectric layers, the RF-TENG shows a superior robustness compared to sliding friction TENG (C-TENG). Fig. 6e compares the surface material abrasion of RF-TENG and C-TENG after 0.12 million rotation cycles. The results show that the metal electrodes of the RF-TENG stay almost intact, while those of C-TENG are worn out. Consequently, the output of the C-TENG dramatically drops to 45% after 2.8 million rotation cycles as shown in Fig. 6d. This further indicates the contribution of the rolling structure on improving robustness, long-term stability and reliability of TENG. Besides, another RF-TENG with similar structure has been developed as shown in Fig. 6f [67]. This proposed device shows excellent reliability in the output performance with less than ±0.5% of current fluctuation after 1.5 million cycles, meanwhile, no significant FEP microstructure abrasion is observed as shown in Fig. 6g.

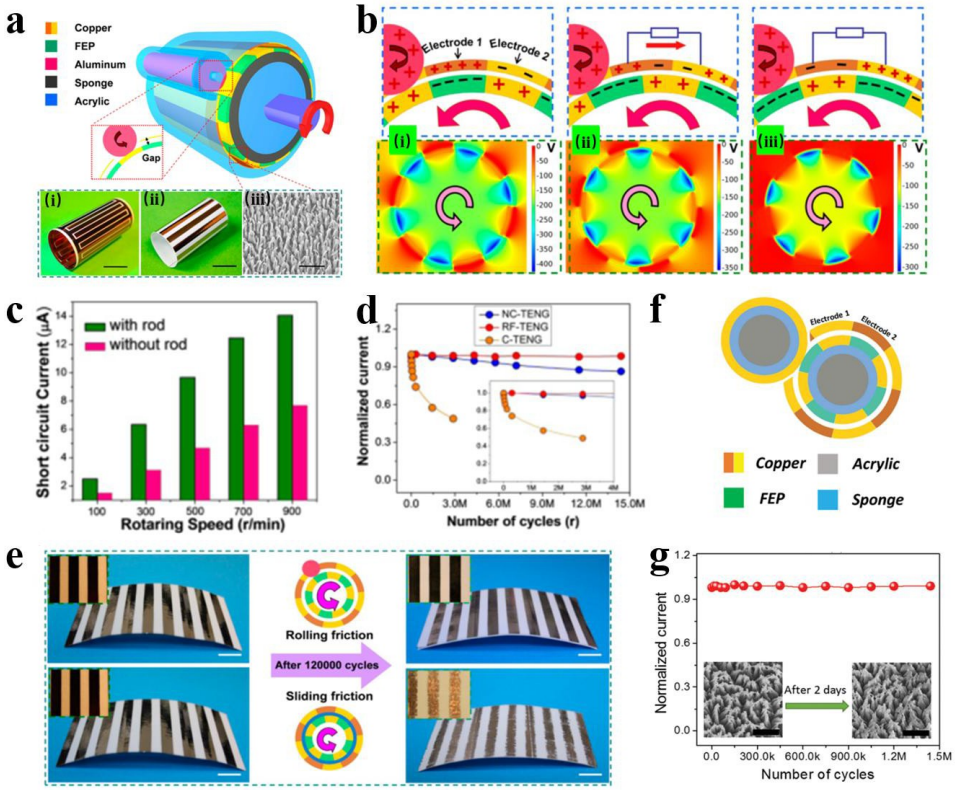

Fig. 6. (a) Structure and (b) working principle of the rolling friction enhanced free-standing mode triboelectric nanogenerator (RF-TENG). (c) Short-circuit current comparison of RF-TENGs with rod rolling friction and NC-TENG without rod rolling friction. (d) Normalized current of RF-TENG, noncontact mode TENG (NC-TENG), and sliding friction TENG (C-TENG) during 14.4 million rotation cycles. (e) Comparison in the metal electrodes abrasion of RF-TENG and C-TENG after 0.12 million rotation cycles. Reproduced with permission from American Chemical Society [66]. (f) Structure schematic of another RF-TENG with similar structure. (g) Stability of output current and FEP surface morphology of this RF-TENG during a continuous operation for 2 days (1.5 million rotation cycles). Reproduced with permission from Wiley-VCH [67].

It has been confirmed that rolling structural TENGs possess obviously improved robustness and durability due to the reduced friction resistance in this structure design. Besides, this approach also avoids some obstacles in noncontact mode TENG, such as performance decrease and electrostatic charge dissipation. The integration of the

rolling structural and noncontact mode TENGs can overcome above obstacles without compromising the device robustness. Nevertheless, the rolling structural TENGs usually require some additional and complicated components, such as barrel, bearings, and rod groups etc., which may bring some limitation for its further application.

4. liquid-solid contact TENGs

Another approach to reduce the abrasion of triboelectric layers is developing liquid-solid contact TENGs [68-74]. Compared to most TENGs relying on the solid-solid contact between triboelectric materials, the liquid-solid contact TENGs produce electricity by the friction between a liquid and a solid surface with much less physical friction resistance. This therefore mitigates the material abrasion and improves the robustness of device. Pan et al. reported a U-tube liquid-FEP-type TENG as illustrated in Fig. 7a [69]. In this design, the FEP U-tube with two Cu electrodes and the inside liquid solution serve as solid and liquid triboelectric materials, respectively. With the swing of the U-tube driven by an external mechanical motion, the internal liquid solution is positively charged due to its different electron affinity with FEP. Similar to a freestanding mode TENG, the reciprocating flowing of charged liquid between the two electrode regions along the inner surface of the FEP tube induces the electric potential difference between electrodes and leads to the generation of electricity as shown in Fig. 7a. Herein, eleven kinds of solution were applied to study the effects of liquid properties on the

device output. Among them, the pure water-FEP U-tube TENG exhibited the best

performance, and therefore was chosen for the follow-up experiments. After continuously measuring the V_{oc} of the water-FEP U-tube TENG for 24 hrs, it is confirmed that this liquid-solid contact device can provide stable output for long time operation with unique advantage as shown in Fig. 7b.

In addition to these freestanding mode liquid-solid contact TENGs, the single-electrode mode liquid-solid contact TENG has also been reported as shown in Fig. 7c [75]. This proposed cylindrical-type water TENG includes a rotating part and a base part with separated superhydrophobic (PTFE coated AAO) and hydrophilic (AAO) layers on its inner surface. With the rotation of the rotating parts, the water inside the cylinder is already positively charged by contacting with the PTFE distributed on the surface of rotating part and superhydrophobic layer. The charged water is pushed and splashed to contact the superhydrophobic and hydrophilic layers with real-time volume change, which causes electric potential difference between the Al electrode and ground (Fig. 7d). Moreover, it should be mentioned that various liquids can be the candidate for fabricating the liquid-solid contact TENGs for different application. For instance, Tang et al. reported a liquid-metal-based triboelectric nanogenerator (LM-TENG) as mechanical energy harvester as shown in Fig. 7e, and their instantaneous energy conversion efficiency can arrive at 70.6% at the best matched load due to the extremely low friction coefficient, large effective contact surface and the electron affinity difference between paired materials [76]. Zhang et al. proposed a self-powered acceleration sensor based on a TENG containing

a liquid metal mercury droplet enclosed in an acrylic shell for vibration detection (Fig. 7f) [77]. The acceleration sensor performs high durability and reliability with negligible performance drop after nearly 200,000 vibration cycles. Additionally, a ferrofluid-based triboelectric-electromagnetic hybrid generator has been reported for vibration energy harvesting as shown in Fig. 7g [78].

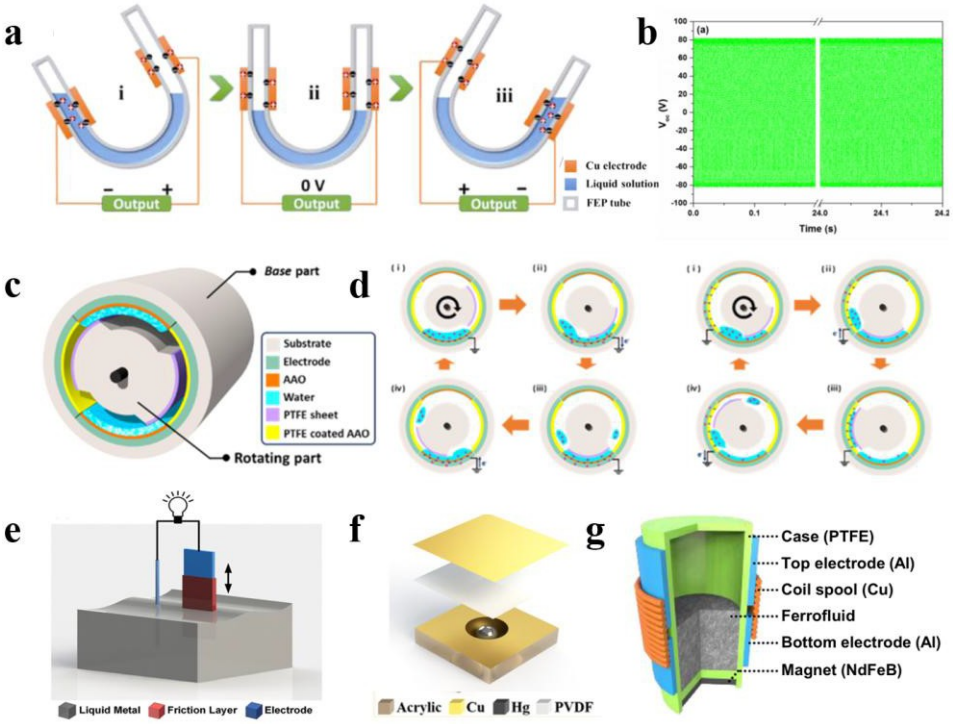

Fig. 7. (a) Structure and working principle of the U-tube liquid-FEP-type TENG. (b) Output voltage of the U-tube liquid-FEP-type TENG during continuous operation for 24 hr. Reproduced with permission from Springer [69]. (c) Structure and (d) working principle of the cylindrical-type water TENG. Reproduced with permission from American Chemical Society [75]. (e) Liquid-metal-based triboelectric nanogenerator (LM-TENG). Reproduced with permission from Wiley-VCH [76]. (f) A self-powered acceleration sensor based on a TENG containing a liquid metal mercury droplet. Reproduced with permission from American Chemical Society [77]. (g) Ferrofluid-based triboelectric-electromagnetic hybrid generator. Reproduced with permission from Elsevier [78].

Generally, the liquid-solid contact TENG is believed to be a simple and applicable method to mitigate the triboelectric materials abrasion. Its another advantage is that it is usually insensitive to humidity, which further improves the reliability of device. Meanwhile, the liquid-solid contact can also arrive at an improved energy conversion efficiency by a more intimate interaction between friction materials. However, some negative factors, such as the unsteadiness of liquid motion especially in strong mechanical impacts, the risk of liquid leakage, and the toxicity of liquid metal etc., should be considered in practical application.

5. Self-recovery TENG

The operation of TENGs requires the device to be long-termly exposed to various mechanical impacts, including not only the external mechanical input but also the physical friction between triboelectric materials. This will increase the probability of material damage and TENG malfunction, leading to the degradation in output performance, reliability and durability of device. In this regard, to develop the self-recovery TENGs with the ability of quickly and conveniently restoring the device performance after device damage is significant for TENG's reliable application [24, 26, 79, 80].

The implementation of healable polymers, one kind of smart material allowing molecular structure repair after fracture, into the TENGs is the most direct and common method to realize the self-recovery of TENGs [23, 24, 81]. Our group reported a fully self-healing TENG by introducing a healable polymer containing

disulfide linkages and the magnetic electrodes consisting of small magnets into the device (Fig. 8a) [24]. The mechanical healability of the healable polymer is evaluated by testing the tensile curve of the original and the healed polymer samples. The results show that the recovery percentage in strain can reach up to 97% after healing the broken specimen at 65 °C for 2 hr as shown in Fig. 8b. For the magnetic electrodes formed by the oriented arrangement of magnetic balls (top electrode) or cubes (bottom electrode), its conductivity can be instantly restored after damage with ignorable resistance fluctuation due to the magnetic attraction as shown in Fig. 8c. The cooperation of healable polymer and magnetic electrodes enables the whole contact-separation mode TENG to be recoverable. Fig. 8d illustrates the I_{sc} of the fully self-healing TENG at original, broken, and healed states, and it is found that the I_{sc} of the healed device can reach up to above 95% of the initial value after five cutting-healing cycles, indicating the device's excellent self-recovery property to meet the requirements in reliability.

Currently, most reported self-healing TENGs need additional stimuli, such as temperature or light, to realize the performance recovery of devices, which limits their realistic application [24, 82-84]. To overcome this boundedness, a self-healable single-electrode mode TENG which can conduct the autonomous healing without external stimuli has been prepared by using a buckled conductive thin electrode sandwiched between two healable PDMS (H-PDMS) films as shown in Fig. 8e [23]. Attributed to the introduction of reversible imine bonds in H-PDMS networks, the

autonomous healing process of the overall device at ambient conditions (21 °C) is well realized, and the mechanical healing efficiency can arrive at 86% in 12 hr (Fig. 8f). Correspondingly, the electrical output performance of the damaged TENG can be almost 100% recovered by means of this autonomous healing process (Fig. 8g).

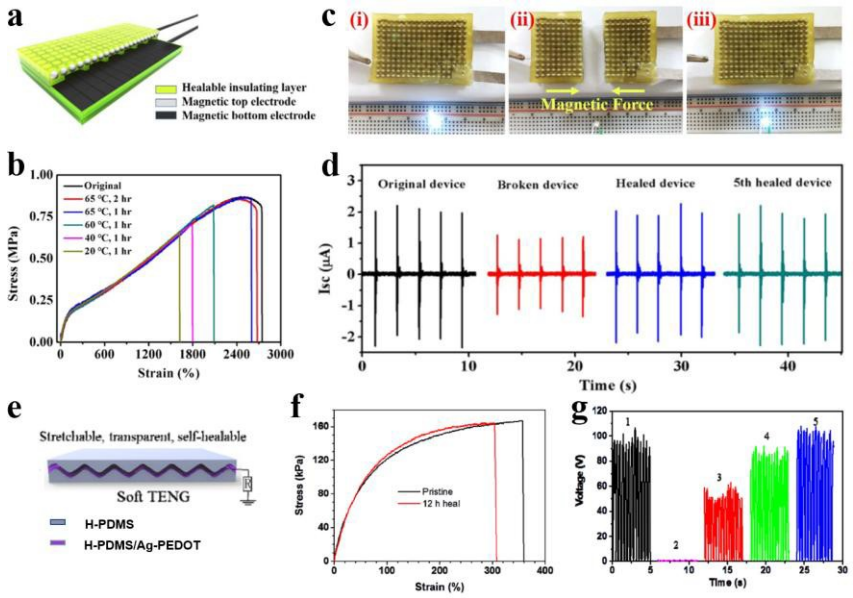

Fig. 8. (a) Structure of the fully self-healing TENG. (b) Stress-strain curves of the healable polymer at original and healed states. (c) Conductivity recovery process of the top magnetic electrode. (d) Output current of the fully self-healing TENG at original, broken, and healed states. Reproduced with permission from Elsevier [24]. (e) Structural schematics of a self-healable single-electrode mode TENG. (f) Stress-strain curves and (g) output voltage of the self-healable single-electrode mode TENG at original and healed states. Reproduced with permission from American Chemical Society [23].

Besides the fracture of the overall device, the performance degradation of TENGs may also be caused by the collapse of micro-structures on triboelectric layer surface under mechanical impacts. These surface micro-structures usually are designed and introduced for enhancing the effective contact area between triboelectric materials, and their collapse thus will obviously decrease the device output. To

achieve the effective recovery of the damaged micro-structure, a few methods have been proposed by using shape-memory polymer (SMP) or photofluidization technology. Lee et al. firstly reported a SMP-based TENG using shape memory polyurethane (SMPU) layer with a micro-pyramid pattern as a triboelectric layer of this contact-separation mode TENG (Fig. 9a and 9b(i)) [80]. After applying a strong impact force of 10 kgf to this SMP-based TENG at room temperature for 15 min, the SMPU pyramid micropattern is flattened (Fig. 9b(ii)), leading to the decrease in V_{oc} of device from initial 80 V to 17 V due to the reduced contact area (Fig. 9c). The degraded device's performance can be recovered once the SMPU is heated to above trigger temperature (55 °C), where the pyramid micropattern restores to its original shape as shown in Fig. 9b(iii), 9c and 9d.

An alternative method to repair morphological damage is using photofluidization technology. Park et al. reported a light-transformable and healable TENG containing a polydisperse orange 3 (PDO 3) triboelectric layer with surface relief gratings (SRGs) as shown in Fig. 9e [85]. The SRGs are inscribed on PDO 3 surface by photofluidic migration process under polarization light irradiation to enable the device to provide a relative high output voltage of 163 V as shown in Fig. 9f(i) and 9g. With the constant mechanical pushing, the SRGs are gradually deformed and collapsed (Fig. 9f(ii)), leading to a performance degradation to 104 V. By means of the reversible photofluidization, the collapsed SRGs could be erased by one beam irradiation with circular polarization (Fig. 9f(iii)) for next re-writing the SRGs on PDO 3 surface by

polarization light irradiation. Correspondingly, the surface morphology of PDO 3 and TENG performance are completely recovered to their initial state as shown in Fig. 9f(iv) and 9g. The application of these methods makes the TENG possess the ability to quickly restore the mechanically damaged device to the normal working state, which extends the lifespan of device and benefits the reliable operation of TENGs in some occasions filled with random and accidental strong mechanical impacts.

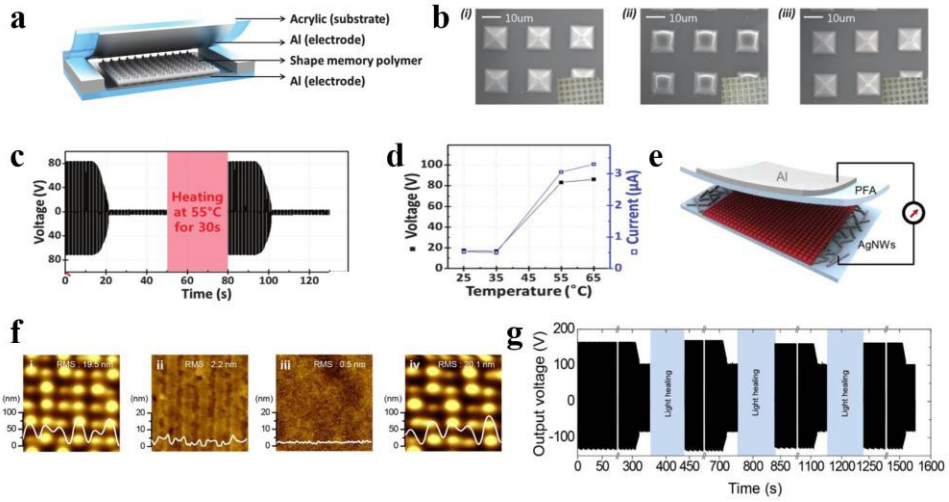

Fig. 9. (a) Structure of the SMP-based TENG. (b) SEM images of the SMP micro-pyramid pattern (i) at initial state, (ii) after deformation by a high compression of 10 kgf, and (iii) after healing process. (c) Open-circuit voltage changes of the SMP-based TENG during the compression-healing process. (d) Open-circuit voltage and short-circuit current change of the SMP-based TENG with the increased healing temperature. Reproduced with permission from Royal Society of Chemistry [80]. (e) Structure of a light-transformable and healable TENG containing a PDO 3 triboelectric layer with surface relief gratings (SRGs). (f) AFM images of the (i) pristine SRGs, (ii) degraded SRGs, (iii) SRGs flattened by one beam irradiation with circular polarization, (iv) SRGs healed by polarization light irradiation. (g) Output voltage change of device during 4 times degradation and light-powered healing cycles of SRGs. Reproduced with permission from Elsevier [85].

Except for mechanical damage, in realistic operation, some other factors, such as dust and other contaminants etc. also lead to the performance degradation of TENGs

by invading triboelectric materials surfaces. In this case, a concept of self-cleaning TENG was proposed to benefit the fast recovery of the contaminated surface. Fig. 10a(i) illustrates a natural lotus leaf-TENG (LL-TENG) fabricated by depositing metal Au on the backside of the dry lotus leaf, and the electricity can be generated by the falling of water droplets on its surface as shown in Fig. 10a(ii) [86]. Given the superhydrophobic property of the natural lotus leaf, the LL-TENG presents the self-cleanability, and the contact layer contaminated by carbon nanopowders can be quickly cleaned after dropping several water droplets onto the dusty surface as shown in Fig. 10b. Taking advantage of this self-cleanability, the contaminated LL-TENG can autonomously restore to the clear appearance and generate the satisfactory I_{sc} without significant performance degradation compared to the initial value as shown in Fig. 10c. This demonstrates its potential for reliable and robust operation in the dusty environment. Additionally, Lee et al. reported another self-cleanable TENG serving as a transparent and attachable ionic communicator (STAIC) [26]. This self-cleanable device consists of a hydrogel with benzophenone treatments as electrode and an external PDMS coating as the contact material. Surface perfluorination on PDMS is conducted by (hepta-decafluoro-1,1,2,2-tetrahydrodecyl) trichlorosilane (HDFS) treatment (Fig. 10d), which makes the device self-cleanable. Fig. 10e-10g compare the self-cleaning behaviors of the non-treated TENG and the HDFS-treated self-cleanable TENG, where the two material surfaces contaminated by activated charcoal powders are successively cleaned by water jet process and ultrasonication

process in ethanol for 10s and 5 min. The results show that the self-cleanable TENG performs a higher recovery efficiency in both transmittance and output voltage to resist external contamination, leading to a more stable, adaptable and reliable application.

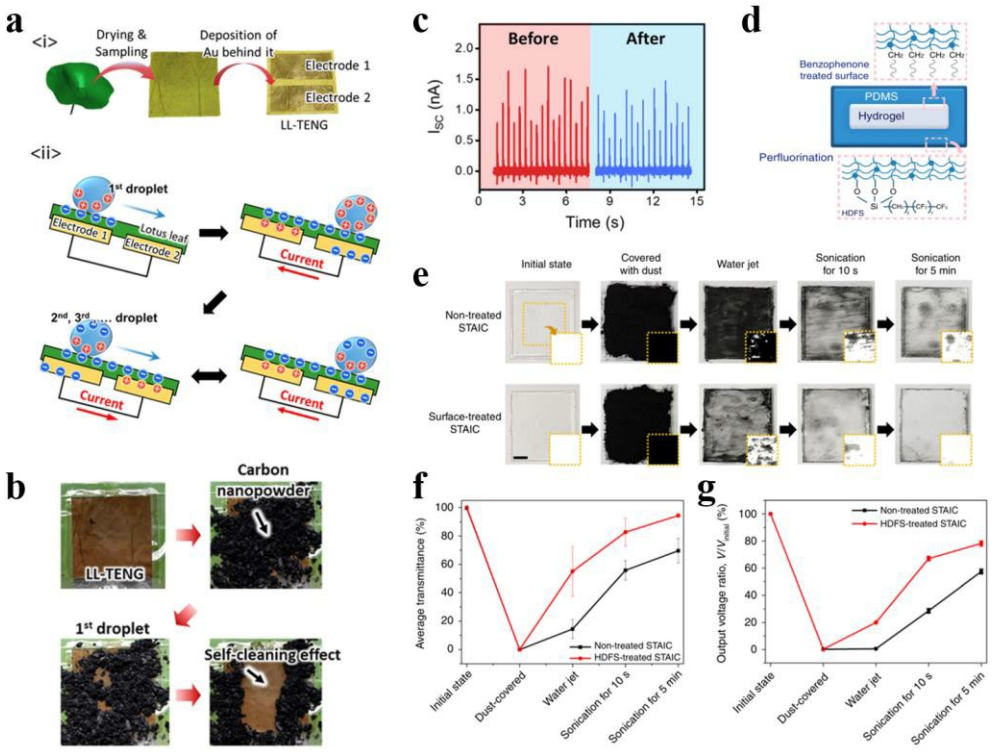

Fig. 10. (a) Fabrication, structure and working principle of the natural lotus leaf-TENG (LL-TENG). (b) Self-cleaning process of the LL-TENG contaminated by carbon nanopowders. (c) I_{sc} of the LL-TENG before contamination occurs and after self-cleaning. Reproduced with permission from Elsevier [86]. (d) Cross-sectional structure of the STAIC. (e) Self-cleanability of HDFS-treated and Non-treated STAICs using activated charcoal powders as contaminant. (f) Average transmittance at 550 nm and (g) output voltage changes of two types of STAICs during the cleaning processes. Reproduced with permission from Nature Publishing Group [26].

Compared to other aforementioned strategies which mainly focus on how to delay device abrasion by reducing the friction resistance, the self-recovery TENG pays more attention to the convenient performance recovery of device once it has

been damaged by mechanical impacts or contaminants. This strategy will extend the life-span of devices and improve the reliability of TENGs in some working occasions filled with accidental strong mechanical impacts and dusts. However, the application of this concept is still limited due to the weak mechanical strength of employed healable or shape-memory polymers themselves.

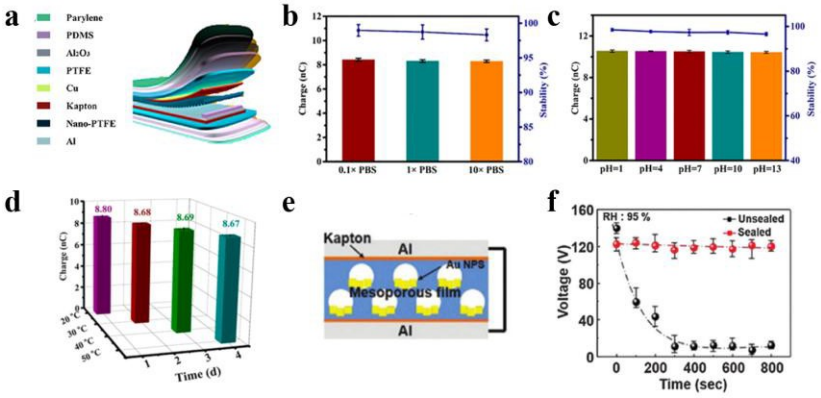

Fig. 11. (a) Schematic of the multilayer packaged TENG. (b)-(d) Transferred charge amount of the multilayer packaged TENG after immersing the device in solution with different concentrations of phosphate buffered saline (PBS) (b), pH value (c), and temperature (d), for over 30 days. Reproduced with permission from American Chemical Society [27]. (e) Device schematic of the Au nanoparticle-embedded mesoporous TENG (AMTENG). (f) The output voltage changes of the unsealed and sealed AMTENGs at a relative humidity of 95% RH. Reproduced with permission from Royal Society of Chemistry [28].

6. Encapsulation of TENG

Since the operation of TENG is based on the triboelectric effect between contact layer surfaces, its performance is largely affected by various environment factors such as humidity, contamination, gas components etc. [26, 27, 57]. These water or impurity molecules as well as dust particles in environment are liable to adhere to the surface

of triboelectric layers and hinder the effective interaction between contact materials, leading to a degradation in the robustness and reliability of TENGs. In this case, the encapsulation of TENGs for separating the contact surface from the outside surrounding will be a feasible strategy to realize a robust and stable operation under harsh conditions.

Zheng et al. demonstrated a multilayer encapsulation process of TENGs to enhance the reliability of device in various harsh environments [27]. As shown in Fig. 11a, a contact-separation mode nude TENG using a nanostructured PTFE and a rough Al sheet as paired frictional layers is encapsulated by multilayer encapsulation materials, including PTFE, PDMS, Aluminum oxide (Al_2O_3) and Paraylene-C. PTFE was chosen as the first encapsulating layer for its good mechanical strength. Tailored PDMS with certain crosslinking degree was then coated onto the PTFE as the second layer to ensure the waterproof capability and structural stability of device. The waterproofness and corrosion resistance were further improved by depositing Al_2O_3 layer onto the PDMS. Finally, a hole-free and high density Parylene-C layer was deposited to provide better anticorrosion performance. The operation reliability of the encapsulated TENG were evaluated by measuring its transferred charge after abusing the device in a series of solutions with different concentrations of phosphate buffered saline, pH value, and temperature for over 30 days as shown in Fig. 11b, 11c, and 11d, respectively. The results show that the multilayer encapsulated TENG remains a stable output with a minor degradation after long-termly working in these harsh

environments, which indicates the feasibility and validity of encapsulation in improving the TENG's reliability and robustness. It is also found that the device can continuously operate for 5 million working cycles with stable output. Making use of the encapsulation process, a series of TENGs with enclosed structure have been fabricated for effectively harvesting energy in real occasions. For instance, Gu et al. proposed a packaged triboelectric nanogenerator (PTNG) enabling noise energy harvesting in dust, humidity, and rainy environments, and the device shows obvious improvement in durability and reliability compared with the unsealed device (UTNG) [87]. Chun et al. compared the electric output of the Au nanoparticle-embedded mesoporous TENGs (AMTENGs) with and without the device sealing process, and it is clearly found that the sealed mesoporous TENG shows a much more stable performance in high humidity of 95% RH as shown in Fig. 11e and 11f [28]. Lee et al. fabricated a fully packaged TENG based on hemispheres-array-structure with excellent mechanical durability, excellent robustness behavior, and high elastic property [88].

The encapsulation of TENGs is mainly related to the enhancement in the reliability of device when using a TENG in harsh environments. Technically, this approach is simple and can be well integrated with other strategies. While, it should be noticed that, sometimes, the properties of encapsulating materials may negatively affect the normal operation of the enclosed TENGs, leading to the degradation in electric output and device functions. Therefore, the design and optimization of

encapsulating materials and processes is necessary to meet the practical application requirement of various devices. Based on aforementioned results, the systematic summary and comparison towards these five types of strategies on improving the robustness and reliability of TENGs are discussed as shown in Table 1. Each strategy performs distinct feature, application scope, and limitation.

Table 1. A comparison about five types of strategies for improving robustness and reliability of TENGs.

	Noncontact mode TENG	**Rolling structural TENG**	**Liquid-solid contact TENG**	**Self-recovery TENG**	**Encapsulation of TENG**
Mechanism	Avoiding contact between triboelectric materials.	Reducing friction resistance.	Reducing friction resistance.	Performance recovery of damaged device.	Isolating triboelectric surfaces from the outside environment.
Pros.	Zero friction resistance, ultra-robust.	Stable output, no electrostatic charge dissipation.	Simple fabrication, high efficiency, insensitive to humidity.	Self repair, compatible to other strategies.	Simple fabrication, Compatible to other strategies, low cost.
Cons.	Output decrease, electrostatic charge dissipation.	Complicated fabrication, limited structure.	Liquid leakage risk, toxicity.	Limited materials choice, low materials bulk strength.	Effect of encapsulating materials on TENGs operation.
Reference	[29] [50] [53]	[61] [63] [66-67]	[69] [72] [76-77]	[23-24] [26] [80]	[27] [87-88]

7. Conclusions and perspectives

In this review, we summarize five types of feasible strategies for improving the robustness and reliability of TENGs. The collective results show that the noncontact mode, the rolling structural and the liquid-solid contact TENGs possess the obviously enhanced robustness due to the reduced friction resistance between triboelectric materials after using these methods. In contrast, the approach of self-recovery TENG pays more attention to the performance recovery of device once it has been damaged

by mechanical impacts or contaminants, which improves the reliability of TENGs, especially, in some working occasions filled with accidental strong mechanical impacts and dusts etc. The encapsulation of TENGs has been proved to be an effective approach to isolate the device from the negative environmental factors for providing a stable and reliable output even in some harsh working conditions. Each strategy performs distinct feature, application scope, and limitation.

Despite many strategies and progress have been achieved to contribute to the improvement of robustness and reliability of TENGs, some challenges and opportunities still exist for future applying and developing these concepts into practical operation. For instance, current approaches mainly focus on enhancing the robustness and reliability of the single TENG itself. However, as a potential alternative to traditional power sources, the integration of considerable TENGs is necessary for large-scale energy harvesting and supply. A good example about this situation is the TENG networks for blue energy harvesting. In this case, besides the single device, the reliability and robustness of the whole TENG networks system also should be considered and improved. Another issue deserving more attempts is to expand the application of TENGs into more various and extreme environments. Although the encapsulation of TENGs has enabled the device to normally work in some moist, dusty, and salt environments, the reliable and robust application of TENGs in some more extreme occasions, such as high temperature, extremely cold, and high radiation districts, still faces severe challenges and need to be deeply and

systematically researched. Thirdly, for some TENGs using polymer electrets as triboelectric materials, both the surface charge density and the output of TENGs can be increased after injecting charges into the material. However, this improvement is remained for only a short period with rapid performance degradation. Some material surface modification technologies, such as inductively coupled plasma (ICP), have presented the ability to delay this degradation to a certain extent by enhancing the triboelectric material's charge storage ability [89]. Despite all this, to realize a durable, stable, and reliable output of this type of device is still an arduous task and deserves more attentions. Additionally, the accelerated life testing should be designed to measure the reliability and robustness of TENGs in a shorter amount of time [90]. Generally, the reliability and robustness are evaluated by measuring the device performance after a continuous operation for certain time or cycles, which will require a long measuring period for overall assessing the device performance during the whole life-span, especially, accompanying with the gradually improved device's robustness. Therefore, to conduct corresponding study on the accelerated life testing based on TENGs is recommended to shorten this process and predict the device performance. Moreover, some limitations in present strategies, including the weak mechanical strength of employed shape-memory and healable polymers themselves, as well as the low safety of the liquid metal etc., should be overcome via material choice and design. Overall, the reliability and robustness of TENGs have been obviously enhanced by means of these highlighted strategies. It is foreseen that the

further progress in these aspects would potentially lead to the extensive andlarge-scale application of TENGs in a variety of occasions.

Acknowledgments

The research was supported by the grants from Research Grants Council of Hong Kong (GRF No. PolyU 153033/17P) and PolyU Grant (G-UABC and 1-ZVGH).

References

[1] S. Shafiee, E. Topal, Energy policy 37 (2009) 181-189.
[2] Z.L. Wang, Nanogenerators for self-powered devices and system, Cham: Georgia Institute of Technology (2011).
[3] D.L. Klass, Biomass for renewable energy, fuels, and chemicals, Cham: Elsevier (1998).
[4] Z.L. Wang, Faraday Discuss. 176 (2015) 447-458.
[5] Z.L. Wang, J. Chen, L. Lin, Energy Environ. Sci. 8 (2015) 2250-2282.
[6] D. Miorandi, S. Sicari, F. De Pellegrini, I. Chlamtac, Ad hoc networks 10 (2012)1497-1516.
[7] F. Achmad, S.K. Kamarudin, W.R.W. Daud, E. Majlan, Appl. Energy 88 (2011)1681-1689.
[8] F.-R. Fan, Z.-Q. Tian, Z.L. Wang, Nano energy 1 (2012) 328-334.
[9] Z.L. Wang, Mater. Today 20 (2017) 74-82.
[10] G. Zhu, B. Peng, J. Chen, Q. Jing, Z.L. Wang, Nano Energy 14 (2015) 126-138.
[11] F.-R. Fan, W. Tang, Y. Yao, J. Luo, C. Zhang, Z.L. Wang, Nanotechnology 25 (2014) 135402.
[12] W. Xu, L.B. Huang, M.C. Wong, L. Chen, G. Bai, J. Hao, Adv. Energy Mater. 7 (2017) 1601529.
[13] Z.L. Wang, ACS Nano 7 (2013) 9533-9557.
[14] G. Zhu, B. Peng, J. Chen, Q.S. Jing, Z.L. Wang, Nano Energy 14 (2015) 126-138.
[15] L.B. Huang, W. Xu, J.H. Hao, Small 13 (2017) 1701820.
[16] M.Y. Ma, Q.L. Liao, G.J. Zhang, Z. Zhang, Q.J. Liang, Y. Zhang, Adv. Funct. Mater. 25 (2015) 6489-6494.
[17] H.S. Wang, C.K. Jeong, M.H. Seo, D.J. Joe, J.H. Han, J.B. Yoon, K.J. Lee, Nano Energy 35 (2017) 415-423.

[18] J.W. Lee, H.J. Cho, J. Chun, K.N. Kim, S. Kim, C.W. Ahn, I.W. Kim, J.Y. Kim, S.W. Kim, C. Yang, J.M. Baik, Sci. Adv. 3 (2017) e1602902.
[19] J.S. Chun, B.U. Ye, J.W. Lee, D. Choi, C.Y. Kang, S.W. Kim, Z.L. Wang, J.M. Baik, Nat. Commun. 7 (2016) 12985.
[20] Z.L. Wang, Triboelectric Nanogenerators, Cham : Springer International Publishing (2016).
[21] J. Chen, Z.L. Wang, Joule 1 (2017) 480-521.
[22] K. Parida, V. Kumar, W. Jiangxin, V. Bhavanasi, R. Bendi, P.S. Lee, Adv. Mater. 29 (2017) 1702181.
[23] J. Sun, X. Pu, M. Liu, A. Yu, C. Du, J. Zhai, W. Hu, Z.L. Wang, ACS Nano 12 (2018) 6147-6155.
[24] W. Xu, L.-B. Huang, J. Hao, Nano Energy 40 (2017) 399-407.
[25] J. Wen, B. Chen, W. Tang, T. Jiang, L. Zhu, L. Xu, J. Chen, J. Shao, K. Han, W. Ma, Adv. Energy Mater. 8 (2018) 1801898.
[26] Y. Lee, S.H. Cha, Y.W. Kim, D. Choi, J.Y. Sun, Nat. Commun. 9 (2018) 1804.
[27] Q. Zheng, Y.M. Jin, Z. Liu, H. Ouyang, H. Li, B.J. Shi, W. Jiang, H. Zhang, Z. Li, Z.L. Wang, ACS Appl. Mater. Interfaces 8 (2016) 26697-26703.
[28] J. Chun, J.W. Kim, W.-s. Jung, C.-Y. Kang, S.-W. Kim, Z.L. Wang, J.M. Baik, Energy Environ. Sci. 8 (2015) 3006-3012.
[29] S. Li, S. Wang, Y. Zi, Z. Wen, L. Lin, G. Zhang, Z.L. Wang, ACS Nano 9 (2015) 7479-7487.
[30] Y. Yu, X. Wang, Extreme. Mech. Lett. 9 (2016) 514-530.
[31] Q. Jing, S. Kar-Narayan, J. Phys. D: Appl. Phys. 51 (2018) 303001.
[32] A.C. Wang, C. Wu, D. Pisignano, Z.L. Wang, L. Persano, J. Appl. Polym. Sci. 135 (2018) 45674.
[33] H. Ryu, S.-W. Kim, Adv. Mater. Lett. 9 (2018) 462-470.
[34] F. Xi, Y. Pang, W. Li, T. Jiang, L. Zhang, T. Guo, G. Liu, C. Zhang, Z.L. Wang, Nano Energy 37 (2017) 168-176.
[35] Z.L. Wang, T. Jiang, L. Xu, Nano Energy 39 (2017) 9-23.
[36] S.H. Wang, L. Lin, Z.L. Wang, Nano Lett. 12 (2012) 6339-6346.
[37] S. Niu, S. Wang, L. Lin, Y. Liu, Y.S. Zhou, Y. Hu, Z.L. Wang, Energy Environ. Sci. 6 (2013) 3576-3583.
[38] J. Zhong, Q. Zhong, F. Fan, Y. Zhang, S. Wang, B. Hu, Z.L. Wang, J. Zhou, Nano Energy 2 (2013) 491-497.
[39] S. Wang, L. Lin, Y. Xie, Q. Jing, S. Niu, Z.L. Wang, Nano Lett. 13 (2013) 2226-2233.
[40] S. Niu, Y. Liu, S. Wang, L. Lin, Y.S. Zhou, Y. Hu, Z.L. Wang, Adv. Mater. 25 (2013) 6184-6193.
[41] G. Zhu, J. Chen, Y. Liu, P. Bai, Y.S. Zhou, Q. Jing, C. Pan, Z.L. Wang, Nano Lett. 13 (2013) 2282-2289.
[42] Y.S. Zhou, G. Zhu, S. Niu, Y. Liu, P. Bai, Q. Jing, Z.L. Wang, Adv. Mater. 26 (2014) 1719-1724.
[43] Y. Yang, H. Zhang, J. Chen, Q. Jing, Y.S. Zhou, X. Wen, Z.L. Wang, ACS Nano 7 (2013) 7342-7351.

[44] Y. Yang, Y.S. Zhou, H. Zhang, Y. Liu, S. Lee, Z.L. Wang, Adv. Mater. 25 (2013) 6594-6601.
[45] B. Meng, W. Tang, Z.-h. Too, X. Zhang, M. Han, W. Liu, H. Zhang, Energy Environ. Sci. 6 (2013) 3235-3240.
[46] F. Yi, L. Lin, S. Niu, P.K. Yang, Z. Wang, J. Chen, Y. Zhou, Y. Zi, J. Wang, Q. Liao, Adv. Funct. Mater. 25 (2015) 3688-3696.
[47] S. Wang, Y. Xie, S. Niu, L. Lin, Z.L. Wang, Adv. Mater. 26 (2014) 2818-2824.
[48] S. Wang, S. Niu, J. Yang, L. Lin, Z.L. Wang, ACS Nano 8 (2014) 12004-12013.
[49] Y. Xie, S. Wang, S. Niu, L. Lin, Q. Jing, J. Yang, Z. Wu, Z.L. Wang, Adv. Mater. 26 (2014) 6599-6607.
[50] L. Lin, S. Wang, S. Niu, C. Liu, Y. Xie, Z.L. Wang, ACS Appl. Mater. Interfaces 6 (2014) 3031-3038.
[51] T. Jiang, X. Chen, K. Yang, C. Han, W. Tang, Z.L. Wang, Nano Res. 9 (2016)1057-1070.
[52] S. Park, H. Ryu, S. Park, H. Hong, H.Y. Jung, J.-J. Park, Nano Energy 33 (2017) 184-194.
[53] H.X. Wu, Z.M. Su, M.Y. Shi, L.M. Miao, Y. Song, H.T. Chen, M.D. Han, H.X. Zhang, Adv. Funct. Mater. 28 (2018) 1704641.
[54] Q. Liang, Z. Zhanga, X. Yan, Y. Gu, Y. Zhao, G. Zhang, S. Lu, Q. Liao, Y. Zhang, Nano Energy 14 (2015) 209-216.
[55] J. Chen, J. Yang, H. Guo, Z. Li, L. Zheng, Y. Su, Z. Wen, X. Fan, Z.L. Wang, ACS Nano 9 (2015) 12334-12343.
[56] L.B. Huang, G. Bai, M.C. Wong, Z. Yang, W. Xu, J. Hao, Adv. Mater. 28 (2016) 2744-2751.
[57] L.-b. Huang, W. Xu, G. Bai, M.-C. Wong, Z. Yang, J. Hao, Nano Energy 30 (2016) 36-42.
[58] X. Ren, H. Fan, C. Wang, J. Ma, S. Lei, Y. Zhao, H. Li, N. Zhao, Nano Energy 35 (2017) 233-241.
[59] H. Yong, J. Chung, D. Choi, D. Jung, M. Cho, S. Lee, Scientific reports 6 (2016) 33977.
[60] D. Kim, I.-W. Tcho, Y.-K. Choi, Nano Energy 52 (2018) 256-263.
[61] L. Lin, Y. Xie, S. Niu, S. Wang, P.-K. Yang, Z.L. Wang, ACS Nano 9 (2015) 922-930.
[62] X. Du, N. Li, Y. Liu, J. Wang, Z. Yuan, Y. Yin, R. Cao, S. Zhao, B. Wang, Z.L. Wang, Nano Res. 11 (2018) 2862-2871.
[63] H. Yang, W. Liu, Y. Xi, M. Lai, H. Guo, G. Liu, M. Wang, T. Li, X. Ji, X. Li, Nano Energy 47 (2018) 539-546.
[64] J. Chen, H. Guo, G. Liu, X. Wang, Y. Xi, M.S. Javed, C. Hu, Nano Energy 33 (2017) 508-514.
[65] X. Wang, Z. Wen, H. Guo, C. Wu, X. He, L. Lin, X. Cao, Z.L. Wang, ACS Nano 10 (2016) 11369-11376.
[66] H. Guo, J. Chen, M.-H. Yeh, X. Fan, Z. Wen, Z. Li, C. Hu, Z.L. Wang, ACS Nano 9 (2015) 5577-5584.
[67] M.H. Yeh, H. Guo, L. Lin, Z. Wen, Z. Li, C. Hu, Z.L. Wang, Adv. Funct. Mater. 26 (2016) 1054-1062.

[68] X. Zhang, Y. Zheng, D. Wang, F. Zhou, Nano Energy 40 (2017) 95-106.
[69] L. Pan, J. Wang, P. Wang, R. Gao, Y.-C. Wang, X. Zhang, J.-J. Zou, Z.L. Wang, Nano Res. 11 (2018) 4062-4073.
[70] T. Kim, J. Chung, D.Y. Kim, J.H. Moon, S. Lee, M. Cho, S.H. Lee, S. Lee, Nano Energy 27 (2016) 340-351.
[71] D. Choi, S. Lee, S.M. Park, H. Cho, W. Hwang, D.S. Kim, Nano Res. 8 (2015)2481-2491.
[72] X. Zhang, Y. Zheng, D. Wang, Z.U. Rahman, F. Zhou, Nano Energy 30 (2016) 321-329.
[73] Q. Shi, H. Wang, H. Wu, C. Lee, Nano Energy 40 (2017) 203-213.
[74] S.-B. Jeon, D. Kim, M.-L. Seol, S.-J. Park, Y.-K. Choi, Nano Energy 17 (2015) 82-90.
[75] S. Lee, J. Chung, D.Y. Kim, J.-Y. Jung, S.H. Lee, S. Lee, ACS Appl. Mater. Interfaces 8 (2016) 25014-25018.
[76] W. Tang, T. Jiang, F.R. Fan, A.F. Yu, C. Zhang, X. Cao, Z.L. Wang, Adv. Funct. Mater. 25 (2015) 3718-3725.
[77] B. Zhang, L. Zhang, W. Deng, L. Jin, F. Chun, H. Pan, B. Gu, H. Zhang, Z. Lv, W. Yang, ACS Nano 11 (2017) 7440-7446.
[78] M.-L. Seol, S.-B. Jeon, J.-W. Han, Y.-K. Choi, Nano energy 31 (2017) 233-238.
[79] K. Parida, V. Kumar, J.X. Wang, V. Bhavanasi, R. Bendi, P.S. Lee, Adv. Mater. 29 (2017) 1702181.
[80] J.H. Lee, R. Hinchet, S.K. Kim, S. Kim, S.-W. Kim, Energy Environ. Sci. 8 (2015) 3605-3613.
[81] Y. Yang, M.W. Urban, Chem. Soc. Rev. 42 (2013) 7446-7467.
[82] J. Deng, X. Kuang, R. Liu, W. Ding, A.C. Wang, Y.C. Lai, K. Dong, Z. Wen, Y. Wang, L. Wang, Adv. Mater. 30 (2018) 1705918.
[83] H.D. Niu, X.Y. Du, S.Y. Zhao, Z.Q. Yuan, X.L. Zhang, R. Cao, Y.Y. Yin, C. Zhang, T. Zhou, C.J. Li, RSC Adv. 8 (2018) 30661-30668.
[84] Q.B. Guan, Y.H. Dai, Y.Q. Yang, X.Y. Bi, Z. Wen, Y. Pan, Nano Energy 51 (2018) 333-339.
[85] J.H. Park, K.J. Park, T. Jiang, Q. Sun, J.-H. Huh, Z.L. Wang, S. Lee, J.H. Cho, Nano energy 38 (2017) 412-418.
[86] D. Choi, D.W. Kim, D. Yoo, K.J. Cha, M. La, D.S. Kim, Nano Energy 36 (2017) 250-259.
[87] L. Gu, N.Y. Cui, J.M. Liu, Y.B. Zheng, S. Bai, Y. Qin, Nanoscale 7 (2015)18049-18053.
[88] K.Y. Lee, H.J. Yoon, T. Jiang, X.N. Wen, W. Seung, S.W. Kim, Z.L. Wang, Adv. Energy Mater. 6 (2016) 1502566.
[89] L. Liu, W. Tang, Z.L. Wang, Nanotechnology 28 (2016) 035405.
[90] W. Nelson, Reliability, IEEE Transactions on R-29 (1980) 103-108.

Personal portrait photo and Biosketch

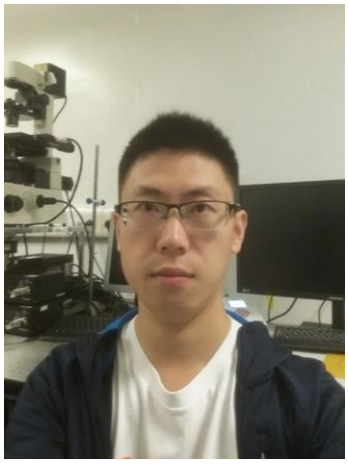

Wei Xu obtained his BSc degree in 2009 from Hefei University of technology. Then he received his Master degree in 2012 from Sichuan University. Now he is a PhD student in Department of Applied Physics under the supervision of Prof. Jianhua Hao. His current research interest is energy harvesting and self-powered system based on functional polymers.

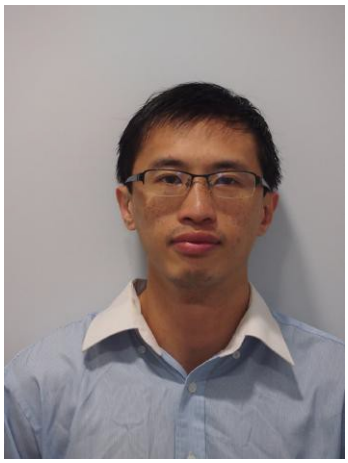

Wong Man Chung received his BS and Master's degree from the Hong Kong Polytechnic University. Now he is pursuing his PhD in Department of Applied Physics in the same university under the supervision of Prof. Jianhua Hao. His current research interests include luminescent materials, smart materials and related hybrid devices.

Prof. Jianhua Hao obtained his BSc, MSc and PhD at Huazhong University of Science and Technology, China. After working at Penn State University, USA, University of Guelph, Canada and the University of Hong Kong, Jianhua Hao joined the faculty in the Hong Kong Polytechnic University (PolyU) in 2006. He is currently a Professor and Associate Head of the Department of Applied Physics in PolyU. Jianhua Hao has published more than 240 papers indexed by ISI Web of Science. His research interests include metal-ion doped luminescent materials and devices, functional thin-films, two-dimensional materials and heterostructures, piezophotonics and nanogenerator (Web Page: http://ap.polyu.edu.hk/apjhhao/).

TOC Graphic:

We review five types of feasible strategies, including noncontact mode, rolling structural, liquid-solid contact, self-recovery and encapsulated TENGs, for the enhancement of robustness and reliability. Some representative examples and their merits are demonstrated to discuss the contribution, availability, and challenges of each strategy.